

Improved mechanical stability of HKUST-1 in confined nanospace

Q1 Q2

M. E. Casco, J. Fernández-Catalá,
M. Martínez-Escamez, F. Rodríguez-Reinoso,
E. V. Ramos-Fernández and J. Silvestre-Albero*

Confinement of HKUST-1 in the cavities of a specially designed activated carbon allows us to improve the mechanical stability of the hybrid system, MOF@AC, while preserving the excellent adsorption properties of the parent MOF.

Please check this proof carefully. **Our staff will not read it in detail after you have returned it.**

Translation errors between word-processor files and typesetting systems can occur so the whole proof needs to be read. Please pay particular attention to: tabulated material; equations; numerical data; figures and graphics; and references. If you have not already indicated the corresponding author(s) please mark their name(s) with an asterisk. Please e-mail a list of corrections or the PDF with electronic notes attached – do not change the text within the PDF file or send a revised manuscript. Corrections at this stage should be minor and not involve extensive changes. All corrections must be sent at the same time.

Please bear in mind that minor layout improvements, e.g. in line breaking, table widths and graphic placement, are routinely applied to the final version.

Please note that, in the typefaces we use, an italic vee looks like this: *v*, and a Greek nu looks like this: ν .

We will publish articles on the web as soon as possible after receiving your corrections; **no late corrections will be made.**

Please return your **final** corrections, where possible within **48 hours** of receipt, by e-mail to: chemcomm@rsc.org

Queries for the attention of the authors





Journal: ChemComm

Paper: c5cc05107j

Title: Improved mechanical stability of HKUST-1 in confined nanospace

Editor's queries are marked on your proof like this , , etc. and for your convenience line numbers are indicated like this 5, 10, 15, ...

Please ensure that all queries are answered when returning your proof corrections so that publication of your article is not delayed.

Query reference	Query	Remarks
Q1 	For your information: You can cite this article before you receive notification of the page numbers by using the following format: (authors), Chem. Commun., (year), DOI: 10.1039/c5cc05107j.	
Q2 	Please carefully check the spelling of all author names. This is important for the correct indexing and future citation of your article. No late corrections can be made.	
	A citation to Fig. 1 has been added here, please check that the placement of this citation is suitable. If the location is not suitable, please indicate where in the text the citation should be inserted.	
	Ref. 9: Can this reference be updated?	

Improved mechanical stability of HKUST-1 in confined nanospace†

Cite this: DOI: 10.1039/c5cc05107j

Received 22nd June 2015,
Accepted 27th July 2015

DOI: 10.1039/c5cc05107j

www.rsc.org/chemcomm

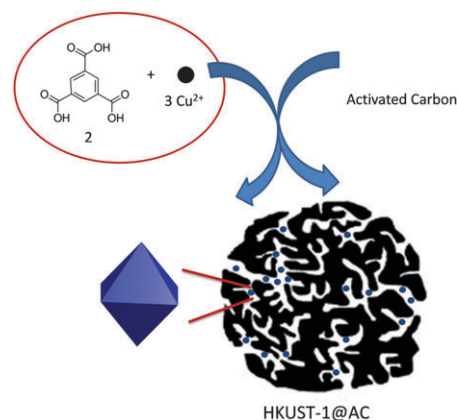
One of the main concerns in the technological application of several metal–organic frameworks (MOFs) relates to their structural instability under pressure (after a conforming step). Here we report for the first time that mechanical instability can be highly improved *via* nucleation and growth of MOF nanocrystals in the confined nanospace of activated carbons.

Metal–organic frameworks (MOFs) have emerged in the last few years as exciting nanomaterials with a very promising performance in a wide range of applications from gas separation and storage,^{1–4} to drug delivery and imaging,^{5,6} and catalysis,^{7–9} among others. Despite the high relevance acquired by MOF materials in the field of nanoporous solids and their applications, these nanoporous materials possess several drawbacks that must be addressed before they can be successfully applied in any industrial technology. One of the main disadvantages of several MOFs concerns their limited structural stability under pressure, *i.e.* the structural damage associated with a mechanical compression required in any conforming step.^{10,11} For instance, recent studies described in the literature have shown that the structural instability of HKUST-1 can give rise to a drastic decrease in the exceptional performance of this MOF for methane storage at high-pressures (up to 50% decrease after a conforming step at 1.5 tons).^{3,12} Consequently, new MOF materials efficiently packable and retaining the full sorption capacity are required for gas storage applications. Besides MOFs, recently published results from our research group have anticipated that carefully designed activated carbons can also be considered as promising porous materials to reach the new DOE target (263 V/V) for methane storage at high pressures but preserving the structural integrity and adsorption properties after a compressing step.¹²

Laboratorio de Materiales Avanzados, Departamento de Química Inorgánica-Instituto Universitario de Materiales, Universidad de Alicante, Ctra. San Vicente-Alicante s/n, E-03690 San Vicente del Raspeig, Spain.
E-mail: joaquin.silvestre@ua.es; Fax: +34 965903454; Tel: +34 965909350

† Electronic supplementary information (ESI) available: Sample preparation and characterization. See DOI: 10.1039/c5cc05107j

M. E. Casco, J. Fernández-Catalá, M. Martínez-Escandell, F. Rodríguez-Reinoso, E. V. Ramos-Fernández and J. Silvestre-Albero*



Scheme 1 Schematic representation of the HKUST-1 nanocrystals grown in the inner cavities of activated carbons.

With this background, the present communication is aimed to take advantage of the privileged structural properties of carbon materials and the exceptional adsorption performance of MOFs *via* nucleation and growth of MOF nanocrystals in the inner cavities of carbon materials (Scheme 1). HKUST-1 was selected as a guest structure for the confinement experiments due to its excellent performance for methane adsorption at high pressures. As a host structure an activated carbon (petroleum-pitch activated carbon-AC) has been specifically designed with a highly developed porous structure (containing micro-/meso- and macropores) so that nano-confinement effects in the cavities of carbon materials can be used.¹³ The main role of the nanocavities, where enhanced adsorption potential emerges, is (i) to promote the growth of MOF nanocrystals and (ii) to protect the guest nanostructures from external stimuli (*e.g.*, mechanical compression). To this end, three hybrid MOF@ACs have been prepared containing 10 wt% (MOF@AC10), 25 wt% (MOF@AC25) and 50 wt% (MOF@AC50) of activated carbon. The synthesis was performed according to the method described by Hupp *et al.* for HKUST-1, but modified by the incorporation of a ranging amount of activated carbon in the reaction media (see the ESI† for further

1 **Table 1** Textural properties deduced from the nitrogen adsorption isotherms at $-196\text{ }^{\circ}\text{C}$ ^a

Sample	$S_{\text{BET}}/\text{m}^2\text{ g}^{-1}$	$V_{\text{DR}}/\text{m}^3\text{ g}^{-1}$	$V_{\text{t}}/\text{cm}^3\text{ g}^{-1}$
HKUST-1	1590	0.51	0.64
MOF@AC10	1700	0.64	0.88
MOF@AC25	1190	0.44	0.86
MOF@AC50	1600	0.51	1.10
AC	3790	1.19	2.40

^a V_{DR} , micropore volume deduced from the Dubinin–Radushkevich equation; V_{t} , total pore volume estimated from the nitrogen adsorption data at $P/P_0 \sim 0.95$.

details).³ It is important to highlight that the hydrothermal synthesis was performed under continuous stirring to minimize reactants' diffusional limitations, thus avoiding preferential growth of the MOF on the external surface of the carbon grains.

Table 1 lists the textural characteristics of the different hybrid systems in terms of BET surface area, micropore volume (calculated using the Dubinin–Radushkevich (DR) equation) and total pore volume (at $P/P_0 \sim 0.95$), estimated from the nitrogen adsorption isotherms at $-196\text{ }^{\circ}\text{C}$ (nitrogen adsorption isotherms and DR plots are shown in Fig. S1a and b, respectively, ESI[†]). Textural properties of the original HKUST-1 and AC are also included for the sake of comparison. As it can be seen in Table 1, the textural parameters of the hybrid systems highly resemble the values of the parent MOF in terms of micropore volume and BET surface area, independently of the amount of carbon incorporated. Although these results are quite surprising, they are highly reproducible for other MOFs evaluated by our research group (e.g. ZIF-8@AC).¹⁴ The observed behaviour could be attributed to the larger skeletal density of MOFs (helium density 2.80 g cm^{-3}), as compared to AC (helium density 1.90 g cm^{-3}), so that the final textural properties per gram of the hybrid system are preferentially defined by the MOF matrix.¹² However, further theoretical calculations will be needed to fully understand this behaviour.

At this point it is important to highlight the sudden decrease observed in the textural parameters of the parent carbon material (mainly S_{BET} , V_{DR} and V_{t}) after a 50 wt% MOF incorporation. This observation clearly suggests that MOF nucleation and growth must take place preferentially in the inner cavities of the activated carbon, although the isolated growth of some MOF crystals on the external surface of the carbon grains cannot be ruled out.

X-ray powder diffraction measurements of the parent MOF show the characteristic peaks associated with HKUST-1 at 2θ : 9.5° , 11.7° and 13.5° , corresponding to (220), (222) and (400) diffraction peaks, respectively. Interestingly, encapsulated HKUST-1 exhibits a similar XRD pattern, i.e. there are no shifts in the peaks' position, although a certain crystallinity loss can be clearly discerned with the amount of carbon incorporated. Despite the similarity in the XRD patterns, it is important to highlight a shift in the relative intensity of the main diffraction peaks of HKUST-1 upon confinement. The (222) diffraction peak experiences a sudden decrease as compared to the (220) and (400) diffraction peaks. This finding may suggest the epitaxial growth of the synthesized nanocrystals in the restricted space of the carbon cavities, this being another sign of the growth of HKUST-1 in the inner cavities of carbon (Fig. 1).

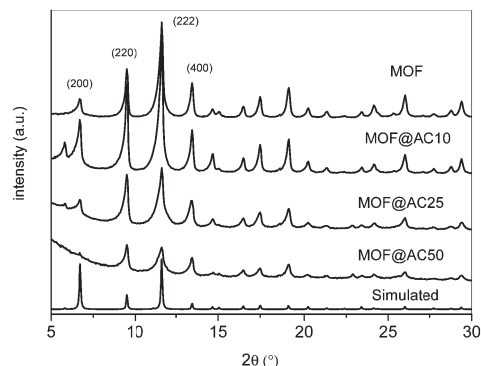


Fig. 1 X-ray diffraction patterns of the different hybrid MOF@AC materials. XRD patterns of HKUST-1 synthesized in this work and simulated spectra¹⁵ are included for the sake of comparison.

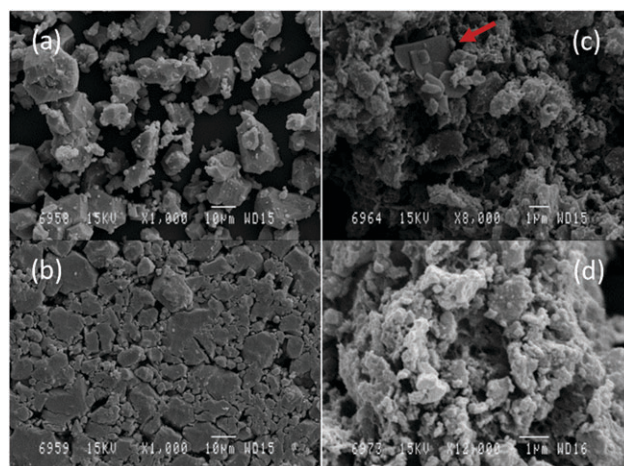


Fig. 2 Scanning electron microscopy images of (a and b) MOF (HKUST-1) and (c and d) MOF@AC (50 wt%) as synthesized (a and c) and after a conforming step at 1.5 tons (b and d).

As described above, the main objective of the present communication is the nucleation and growth of HKUST-1 in the cavities of activated carbons to prevent any structural damage or collapse after a mechanical stress. To this end, Fig. 2 compares the morphological changes of the original HKUST-1 sample and the hybrid MOF@AC50 system, as synthesized (a and c), and after a conforming step at 1.5 tons (b and d). The original HKUST-1 presents a heterogeneous particle size distribution with an average crystal size around 360 nm, as deduced from the (222) peak in the XRD measurements using Scherrer's equation. It is worth mentioning that the particle size obtained under stirring conditions is smaller to that obtained in the conventional synthesis described in ref. 3.

A conforming step at 1.5 tons (see Fig. 2) gives rise to a compaction of the nanocrystals accompanied by a sudden deterioration in the crystal structure, in close agreement with previous observations.^{3,12} The deterioration of the MOF crystal structure after a conforming step is also confirmed by comparing the XRD profiles (see Fig. S2, ESI[†]).

Concerning the hybrid system, scanning electron microscopy (SEM) images show the carbon matrix (carbon particle

size *ca.* 1–10 μm) and the MOF nanocrystals (red arrow) growing preferentially in the larger cavities (large macropores). Unfortunately, SEM does not provide information about the scenario that took place in narrower pores (mesopores and micropores), where MOF growth is expected (as deduced from N_2 adsorption measurements). The hybrid sample subjected to a mechanical stress of 1.5 tons (Fig. 2d) does not reflect any morphological change or damage, in close agreement with the high structural stability and rigidity of activated carbons as compared to MOFs. The higher stability of the hybrid systems can be clearly appreciated in the XRD patterns obtained after the conforming step (Fig. S2, ESI †).

Another important parameter define the structural stability of nanoporous materials under mechanical stress concerns their textural properties. Fig. 3 compares the nitrogen adsorption isotherms at -196°C for the (a) HKUST-1 sample and (b) hybrid MOF@AC50 after a mechanical compression at 0.5, 1 and 1.5 tons. As described in our previous studies, the original MOF exhibits significant structural instability associated with progressive damage to the porous structure under external mechanical pressure. For instance, the BET surface area of the HKUST-1 sample exhibits a decrease of 43% ($900\text{ m}^2\text{ g}^{-1}$ vs. $1590\text{ m}^2\text{ g}^{-1}$) upon mechanical conforming at 1.5 ton, thus confirming the partial collapse of the crystal structure, in close agreement with SEM images.

A completely different scenario accounts for the hybrid samples (*e.g.*, MOF@AC50). The nitrogen adsorption isotherm of the parent hybrid MOF@AC50 system exhibits type IV, according to the IUPAC classification, clearly resembling that of the host activated carbon (see Fig. S1, ESI †), although with a smaller total adsorption capacity (55% reduction in the total pore volume of the host AC after MOF

incorporation). Interestingly, a subsequent conforming step up to 0.5, 1.0 and 1.5 tons has no effect on the textural properties of the sample. BET surface area, and micro- and total pore volume remain mainly unchanged within the experimental error. This observation clearly anticipates for the first time the synergistic effect between activated carbons and MOFs, *i.e.* the protective role of the carbon nanocavities in the growth of MOF nanocrystals in their bed while preserving the textural properties and adsorption performance of the original MOF (see Fig. S3, ESI †).

Another proof of the presence of HKUST-1 encapsulated in the pores of the host carbon material can be obtained from the textural parameters obtained from the nitrogen adsorption measurements. If all the HKUST-1 is outside the carbon material, the total pore volume for MOF@AC50 detected by nitrogen would be $V_t = 0.5 \times V_{\text{AC}} + 0.5 \times V_{\text{MOF}} = 0.5 \times 2.40 + 0.5 \times 0.64 = 1.52\text{ cm}^3\text{ g}^{-1}$, which is far from the obtained value ($V_t = 1.10\text{ cm}^3\text{ g}^{-1}$). In contrast, if all HKUST-1 is inside the cavities of the host carbon material, the total adsorption capacity of the carbon must decrease according to the MOF density ($\rho = 0.88\text{ g cm}^{-3}$) but considering the additional contribution from the MOF to the total adsorption capacity, *i.e.* $V_2 = (0.5 \times V_{\text{AC}} - 0.5/\rho) + 0.5 \times V_{\text{MOF}} = (0.5 \times 2.40 - 0.5/0.88) + 0.5 \times 0.64 = 0.95\text{ cm}^3\text{ g}^{-1}$, in close agreement with the experimental value. This statement confirms that the majority of the HKUST-1 crystals must be located inside the cavities of the carbon material.

Last but not least, these hybrid materials were evaluated in the adsorption of methane at 25°C and high-pressure (up to 10 MPa), before and after a conforming step. As described in Fig. 4, HKUST-1 (MOF) exhibits a considerable adsorption capacity for methane reaching saturation at around 8 MPa with a final value of 0.16 g g^{-1} . It is worth mentioning that the amount adsorbed on the HKUST-1 material used in this manuscript is smaller than the previous values reported in the literature.^{3,12} The lower adsorption capacity of methane on the present sample must be attributed to the smaller crystal size (due to the stirring during the synthesis), thus anticipating the critical role of the crystal size in methane storage in HKUST-1 at high pressures. Confinement of HKUST-1 in the cavities of the activated carbons gives rise to a minor decrease in the excess methane adsorption capacity, mainly at moderate pressures, while the final value at 10 MPa of the amount adsorbed resembles that of the parent MOF (see Table S1 for compilation of the adsorption data, ESI †).

A completely different situation takes place after a conforming step at 1 ton. As observed in Fig. 4b, the excess methane adsorbed drastically drops in the non-confined MOF down to 0.05 g g^{-1} , in close agreement with previous observations.^{3,12} However, the detrimental effect of a mechanical stress decreases with the amount of carbon in the hybrid system up to sample MOF@AC50, with mainly no effect on the amount of methane adsorbed at 10 MPa (0.14 g g^{-1} vs. 0.15 g g^{-1}). These results constitute the first proof-of-concept for MOF protection against external stimuli (*e.g.*, pressure required for a conforming step), *via* confinement of the MOF in the nanocavities of activated carbons while preserving the adsorption properties of the non-confined nanocrystals.

To end up, Table 2 compares the excess methane adsorption capacity on volumetric basis (V/V) for the different samples

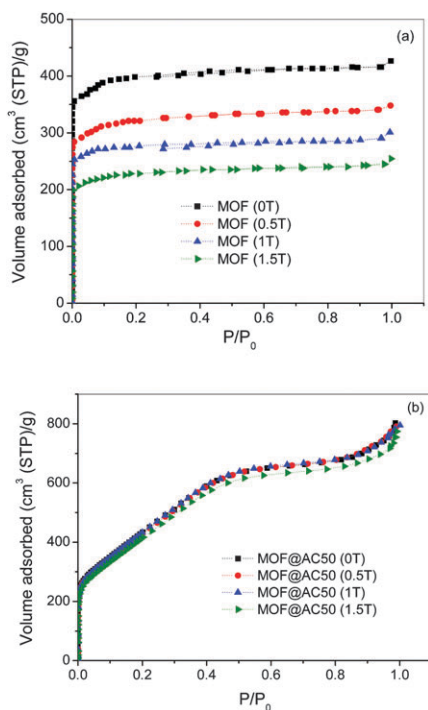


Fig. 3 Nitrogen adsorption/desorption isotherms of (a) MOF and (b) MOF@AC (50 wt%), after a conforming step at 0, 0.5, 1 and 1.5 tons.

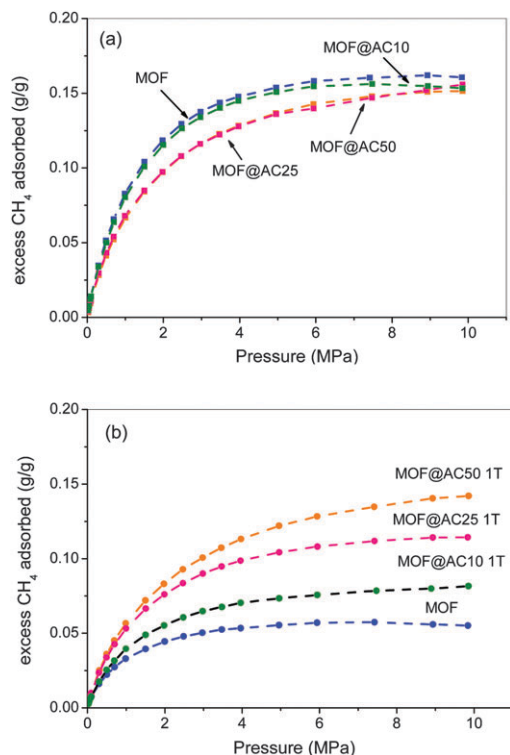


Fig. 4 Excess methane adsorption isotherms at 25 °C in the hybrid MOF@AC samples (a) as synthesized and (b) after a conforming step at 1 ton.

Table 2 Excess methane uptake at 10 MPa and 25 °C for the different samples before and after the conforming step. Volumetric capacity (V/V) has been calculated using the bulk density measured at 1.0 ton (also included in the Table S1, ESI)

Sample	ρ^a (g cm ⁻³)	Excess methane (10 MPa, 25 °C)	Excess methane ^b (10 MPa, 25 °C)
MOF	0.88	198 V/V	68 V/V
MOF@AC10	0.83	179 V/V	95 V/V
MOF@AC25	0.75	163 V/V	119 V/V
MOF@AC50	0.63	134 V/V	126 V/V

^a Bulk density measured at 1.0 ton. ^b Excess methane after a conforming step at 1.0 ton.

before and after the compressing step. As expected, differences in the methane adsorption capacity become larger among samples on volumetric basis as compared to that on gravimetric basis, due to the higher density of HKUST-1 vs. the hybrid systems.

The excess methane adsorbed in the as-synthesized samples decreases with the amount of carbon incorporated from 198 V/V down to 134 V/V (using erroneously the bulk density measured at 1.0 ton when the sample is already damaged). As described before, the volumetric adsorption capacity is larger for the large crystals of HKUST-1 (257 V/V according to our previous measurements in ref. 10), as compared to the new sample prepared under stirring conditions. In the same way as before, the scenario changes drastically after the conformation of the different samples.

The non-confined MOF suffers dramatic reduction in the excess methane adsorption capacity down to 68 V/V, whereas the confined samples (preferentially the MOF@AC50 sample) do not. At this point it is important to emphasize that despite these advantages, hybrid MOF@AC systems will never outperform the adsorption performance of the parent MOF, at least in crystal size dependent applications such as methane adsorption, due to the hindered growth of the MOF in the restricted nanospace of carbon cavities.

In summary, this manuscript describes the nucleation and growth of HKUST-1 nanocrystals in the cavities of carefully designed activated carbon materials. Gas adsorption measurements suggest that nucleation and growth of MOF nanocrystals must take place preferentially in the confined nanocavities of the carbon material, as confirmed by microscopy. Confinement of MOF nanocrystals provides a considerable improvement in the mechanical properties of the MOF due to the protective barrier of the host carbon against a mechanical stress, while preserving the excellent adsorption properties of the guest MOF. Whereas the porous structure of the isolated HKUST-1 sample exhibits drastic structural collapse after a mechanical stress of 1 ton, hybrid systems are able to withstand higher pressures without any significant modification in the adsorption properties of the confined MOF.

Financial support from MINECO projects MAT2013-45008-p and CONCERT Project-NASEMS (PCIN-2013-057) is gratefully acknowledged.

Notes and references

- 1 K. Sumida, D. L. Rogow, J. A. Mason, T. M. McDonalds, E. D. Bloch, Z. R. Herm, T.-H. Bae and J. R. Long, *Chem. Rev.*, 2012, **112**, 724.
- 2 A. R. Millward and O. M. Yaghi, *J. Am. Chem. Soc.*, 2005, **127**, 17998.
- 3 Y. Peng, V. Krungleviciute, I. Eryazici, J. T. Hupp, O. K. Farha and T. Yildirim, *J. Am. Chem. Soc.*, 2013, **135**, 11887.
- 4 I. Senkowska and S. Kaskel, *Microporous Mesoporous Mater.*, 2008, **112**, 108.
- 5 P. Horcajada, C. Serre, G. Maurin, N. A. Ramsahye, F. Balas, M. Vallet-Regi, M. Sebban, F. Taulelle and G. Férey, *J. Am. Chem. Soc.*, 2008, **130**, 6774.
- 6 P. Horcajada, T. Chalati, C. Serre, B. Gillet, C. Sebrie, T. Baati, J. F. Eubank, D. Heurtaux, P. Clayette, C. Kreuz, J.-S. Chang, Y. K. Hwang, V. Marsaud, P.-N. Bories, L. Cynober, S. Gil, G. Férey, P. Couvreur and R. Gref, *Nat. Mater.*, 2010, **9**, 172.
- 7 J. Y. Lee, O. K. Farha, J. Roberts, K. A. Scheidt, S. T. Nguyen and J. T. Hupp, *Chem. Soc. Rev.*, 2009, **38**, 1450.
- 8 J. Gascon, A. Corma, F. Kapteijn and F. X. Llabrés i Xarxa, *ACS Catal.*, 2014, **4**, 361.
- 9 B. Gole, U. Sanyal and P. S. Mukherjee, *Chem. Commun.*, 2015, **10.1039/c4cc09228g**.
- 10 J. Chong Tan and A. K. Cheetham, *Chem. Soc. Rev.*, 2011, **40**, 1059.
- 11 T. Tian, J. Velazquez-Garcia, T. D. Bennett and D. Fairen-Jimenez, *J. Mater. Chem. A*, 2015, **3**, 2999.
- 12 M. E. Casco, M. Martínez-Escandell, E. Gadea-Ramos, K. Kaneko, J. Silvestre-Albero and F. Rodríguez-Reinoso, *Chem. Mater.*, 2015, **27**, 959.
- 13 M. E. Casco, J. Silvestre-Albero, A. J. Ramirez-Cuesta, F. Rey, J. L. Jorda, A. Bansode, A. Urakawa, I. Peral, M. Martínez-Escandell, K. Kaneko and F. Rodríguez-Reinoso, *Nat. Commun.*, 2015, **6**, 6432.
- 14 M.E. Casco, D. Fairen-Jimenez, A.J. Ramirez-Cuesta, L. Daeman, E.V. Ramos-Fernandez, J. Silvestre-Albero, unpublished results.
- 15 Simulated XRD patterns obtained from <http://www.crystallography.net/cod/2300380.html>, accessed on July 14th 2015.